1. Title page

Vestibulocollic and cervicocollic muscle reflexes in a finite element neck model during multidirectional impacts

Abbreviated title: Neck reflexes model in multidirectional impacts

Matheus A. Correia[1], Stewart D. McLachlin[1], Duane S. Cronin[1*]

[1]Department of Mechanical Engineering, University of Waterloo, 200 University Avenue West, Waterloo, Ontario, Canada N2L 3G1

*Tel.: +1 519 888 4567x32682. dscronin@uwaterloo.ca

2. Abstract and Keywords

Active neck musculature plays an important role in the response of the head and neck during impact and can affect the risk of injury. Finite element Human Body Models (HBM) have been proposed with open and closed-loop controllers for activation of muscle forces; however, the controllers in many current models are often calibrated to specific experimental loading cases, without considering the intrinsic role of physiologic muscle reflex mechanisms under different loading conditions. The goal of this study was to develop a closed-loop controller for a contemporary male HBM to represent muscle activation mechanisms based on the vestibulocollic and cervicocollic reflexes. Dual PID controllers were implemented, with head rotation and muscle stretch used for input. Controller parameters were optimized using volunteer data and then independently assessed across twelve impact conditions. The kinematics from the closed-loop controller simulations showed good average correlations to the experimental data (0.699) for the impacts. Compared to a previous optimized open-loop activation strategy, the average difference was less than 9%. The incorporation of the reflex mechanisms using a closed-loop controller can provide robust performance for a range of impact directions and severities, which is critical to improving HBM response under a larger spectrum of automotive impact simulations.

Keywords: Muscle activation, vestibulocollic reflex, cervicocollic reflex, human body model, finite element method, head kinematics, neck model

3. Introduction

The natural reflex mechanisms of the cervical musculature play an important role in the stabilization of the head and neck[34], increasing the stiffness of the neck column and potentially influencing the risk of injury under impact conditions, particularly for lower severity impacts.[46] Rising interest to develop active safety systems in the automotive industry has increased the need to better understand the role of active musculature contraction during the impact response of the human body. Post-mortem human subjects (PMHS) and anthropometric testing devices (ATD), commonly used to assess risk of injury for vehicle safety tests, cannot represent physiologic muscle activation.[3,20,46] As occupants in real-life crash scenarios could have their kinematic response altered by muscle activation, vehicle safety tests may be limited when extrapolating post-mortem results.[1] Characterizing this phenomenon under a range of conditions, from low severity accelerations in autonomous braking to high severity frontal impacts, is not experimentally feasible and an alternate approach is required.

Computational finite element (FE) Human Body Models (HBM) can be used to predict the response and potential injury risk following impact; yet, the efficacy of these models depends on the underlying implementation of human physiology. In general, active musculature implementations in HBM use pre-defined muscle activation parameters for open-loop control of muscle onset time and activation level.[10] However, an open-loop approach limits the robustness of the model to effectively adapt to different impact scenarios or requires optimization to specific impact scenarios. Implementation of a closed-loop control approach could enable automation of the muscle activation allowing for adaptation of the parameters to suit different impact scenarios.[37]

Closed-loop control for muscle activation has typically been implemented using a proportional–integral–derivative (PID) controller with feedback based on global kinematics, such as the head center of gravity rotational angle.[22,41] The parameters for these closed-loop controllers are usually calibrated to specific experimental loading cases using inverse methods, reducing their generalizability to adapt to different loading conditions. This limitation is largely due to a lack of electromyography (EMG) data for higher severity impacts (>8g), which has created a gap in understanding the role and complex interactions between different muscle activations during these events.[29]

Muscle Activation

Muscle tissue can produce both a passive restorative force and an active force. The passive force is intrinsic to the muscle without activation, exhibiting viscoelastic and anisotropic characteristics, as expected for biological tissues with fibers.[2,6,31,48] Passive response behavior has been modeled numerically using a linear-viscoelastic formulation, such as an Ogden formulation.[17] In contrast, active muscle force is controlled by nerve impulses originating in the central nervous system and transmitted through motor neurons to the actuating cells, being a function of the muscle length and rate of change in length. In response to this stimulus, the contraction is developed by the intracellular structure (sarcomeres) through sliding filaments of actin and myosin parallel to the longer dimension of the muscle fibers. The Hill-type active muscle model is a widely used approach to model muscle activation and the resulting contractile force[4,25], and is implemented in many commercial FE codes, often using two-dimensional elements joining two points to represent the muscle. The activation of the muscle in this formulation is represented by a curve describing the magnitude of activation with respect to time. A recent study identified optimized activation onset times for the flexors and extensors muscles in the neck using experimental data from a series of rear impacts and frontal impacts sled tests conducted with volunteers.[10] The use of optimized muscle activation curves was found to improve the resulting head kinematics of a detailed FE head and neck models over a wide range of impact severities in comparison to the best available data.[10] These optimized muscle activation onset times and magnitudes can provide guidance for the implementation of a more robust closed-loop controller of the cervical muscles.

Muscle Reflex Mechanisms

An important physiologic factor for the development of a closed-loop muscle activation controller is the natural human reflex mechanisms. The vestibulocollic reflex (VCR) and cervicocollic reflex (CCR) are primarily responsible for head and neck stabilization and, therefore, a crucial focal point for muscle activation during impact.[16,40,41,43]

The VCR system receives input from the semicircular canals and cochlea in the inner ear, with a delayed onset time relative to the external stimulus and is directly related to the angular and linear accelerations of the head. The CCR receives signals from modified muscle fibers diffusely distributed in the muscles and presents a fast onset time, with muscle stretch and stretch rate as the input. The CCR is activated in two stages, a fast initial response and a slower later response that can be related to the head rotation magnitude (θ) (Figure 1).[40]

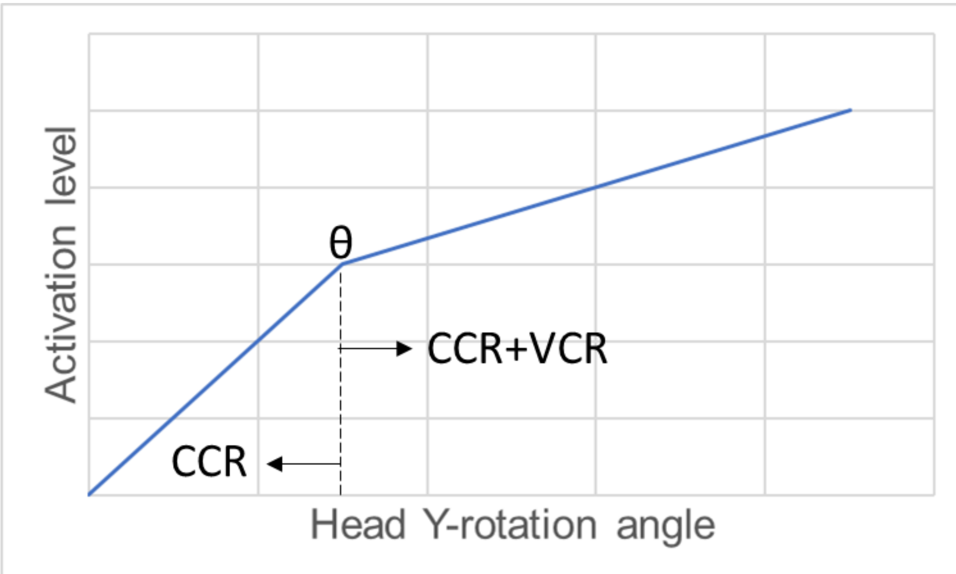

Figure 1: Idealized muscle activation, based on electromyographic (EMG) measurements, due to the combination of cervicocollic (CCR) and vestibulocollic reflexes (VCR) versus the head rotation angle. Before a head rotation angle of θ is reached mainly CCR is active, after which a combination of VCR and CCR are active.

Experimental Impact Data

Validation of computational models representing physiologic muscle activation patterns using available experimental data presents several challenges. Diverse experimental studies have investigated car and sled tests with volunteers in low severity autonomous braking and impacts (1g to 4g) and reported the effect of muscle activation on the response.[9,11,14,18,26,33,45] Relevant conclusions have included an observed increase in the neck muscle activation during impacts, a higher angular head rotation for females during impacts, as well as challenges in terms of measuring muscle activation magnitudes using normalized EMG data. Further, many of these studies have not reported important experimental boundary conditions (i.e. seat inclination, presence of headrest, etc.), making it difficult to reproduce the experiments in a simulation environment or to quantify the effects of muscle activation.

An experimental dataset containing a wide range of volunteer impact severities[32] conducted by the Naval Biodynamics Laboratory (NBDL) includes head and neck kinematic data. Data were collected from 16 volunteers subjected to 119 frontal and 72 lateral impact sled tests.[47,50] The experimental peak accelerations ranged from 2g to 15g and demonstrated low variability within a specific impact condition, owing to the restraint system used in the experiments. A limitation of the experimental data was that no measurements of the volunteer's muscle activation were recorded during the impact tests. There is a scarcity of higher severity rear impact studies owing to volunteer injury risk. One detailed rear impact study was performed over a series of 3g and 4g sled tests[35,44] with 12 human volunteers used to assess the global head kinematics response. The rear impact tests in this study did not include a headrest so that free motion of the head could be assessed; however, muscle activation levels were not measured during the tests.

HBMs with Active Musculature

Neck muscle activation has been examined in FE HBM including the Global Human Body Models Consortium (GHBMC), Royal Institute of Technology model (KTH), Japan Automobile Manufacturers Association model (JAMA), Total Human Model for Safety

(THUMS), and simTK models.[8,12,21,49] Considering contemporary HBM, only the GHBMC and THUMS models incorporate a combination of skin, adipose tissue, 3D passive muscles, and active 1D muscles. The soft tissues are relevant for the head and neck kinematics because of the increase in stiffness of the system resulting from these tissues. Specifically, the GHBMC neck model has been assessed and validated in a hierarchical manner at the motion segment[5] and full neck levels[4], and optimized open-loop muscle activations strategies have shown good correspondence to human volunteer data.[10] The model was developed from MRI and CT scans of a living 26-year-old adult with the anthropometrics of a mid-size male.[51]

The GHBMC 50th percentile male (M50-O v5.1) head and neck model used in this study was extracted from the full human body model (Figure 2) and includes 1D Hill-type elements representing the active portion of the muscles and 3D solid hexahedral elements with a hyperelastic material constitutive model representing the passive response of the muscle. The passive and active elements were connected to one another through a series of one-dimensional attachments or support elements to maintain connectivity and the line of action of each muscle.[4]

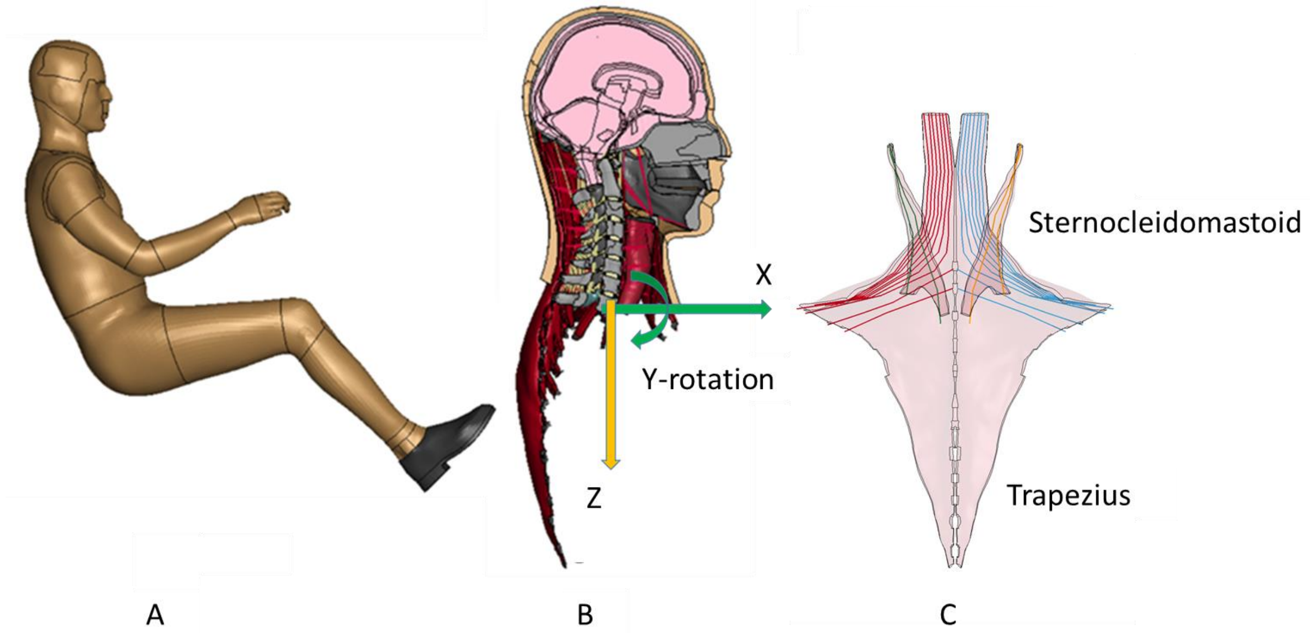

Figure 2: A) GHBMC 50th percentile male full human body model. B) Head and neck model with T1 coordinate system and muscle attachments. C) Frontal view of the 3D passive component (transparent geometry) of the trapezius and sternocleidomastoid with the embedded active Hill-type elements (colored lines).

The GHBMC average stature male model incorporates open-loop controls for the muscles with predefined muscle activation curves that mimic the muscle reflexes in a prescribed manner. The older versions of the model include an open-loop muscle activation scheme, defined as the Maximum Muscle Activation (MMA)[4], corresponding to a neuronal impulse (step signal) of 100% for 100ms generating a maximum value of the activation function in the muscle of 0.871[38]. The onset time for this activation was 74ms, an average of the values presented in the literature for a series of tests with volunteers[38]. In a recent study, two additional open-loop muscle activation strategies were proposed[10]: Cocontraction Muscle Activation (CMA) and Optimized Muscle Activation (OMA). The CMA had a generalized activation of 100% for flexors and 20% for the extensors representing a muscle contraction that would minimize head rotation when no other load was applied, based on simulation of a startle reflex. The OMA consisted of a specific activation curve for each simulated impact direction and severity, obtained from an optimization process of the muscle activation parameters to best achieve the average resultant head kinematics reported in the experimental data. However, closed-loop controllers present an opportunity to more effectively and efficiently address a wider range of impact severities and directions. A number of closed-loop controllers have already demonstrated promising results to simulate natural muscle reflexes.[21,23,36,39] Current implementations based on the head rotation angle with respect to T1 and the muscle spindle response[22,41,42,52] have provided head kinematics with good correlation to the experimental data for specific scenarios. A recent model incorporating a VCR and CCR feedback controller was fitted to experimental data for studying neck stabilization[16], but only assessed for accelerations lower than 1g without consideration for the higher accelerations from impact scenarios. Further, the general applicability of these models is often limited as the controller parameters are often calibrated to specific impact scenarios without examining the performance of the controller against uncalibrated data sets.

The goals of the current study were to: (1) develop a closed-loop controller for neck muscle activation based on the VCR and CCR reflex responses using a small subset of frontal impact conditions from human volunteer data to optimize the controller parameters, and (2) assess the performance of the controller using the frontal impact calibration data and uncalibrated human volunteer data from 12 scenarios representing three impact directions over a range of impact severities.

4. Materials and Methods

The head and neck of a validated average male detailed HBM (M50-O v5.1, 50th percentile, GHBMC) (Figure 2) were extracted for the purposes of assessing the activation controller. The extracted model included the neck musculature, represented by passive 3D and active 1D Hill-type elements, the cervical vertebrae (C1 to C7), the first thoracic vertebra (T1), cervical spine ligaments, intervertebral discs, and skin. The cervical muscles in the model were grouped into four sets according to the respective anatomical region: the left extensors, the right extensors, the left flexors, and the right flexors (Figure 3). The axis system used as the global frame of reference had the X direction pointing forward, Y direction pointing to the left, and Z direction pointing downwards.

Nine different frontal impact severities were simulated, ranging from 2g to 15g corresponding to the NBDL volunteer frontal impact sled test maximum accelerations[13,47], for a total duration of 250ms. The NBDL experimental head kinematics were reported for individual cases; in the current study, head kinematics were averaged for all test subjects for a specific sled acceleration for comparison to the model output. The average response and standard deviation for each impact severity were calculated using point-wise analysis for each case within a specific impact severity.[4] The average linear forward X-acceleration and Y-rotational displacement measured at the first thoracic vertebra (T1) in the volunteer experiments were applied to the T1 in the model.

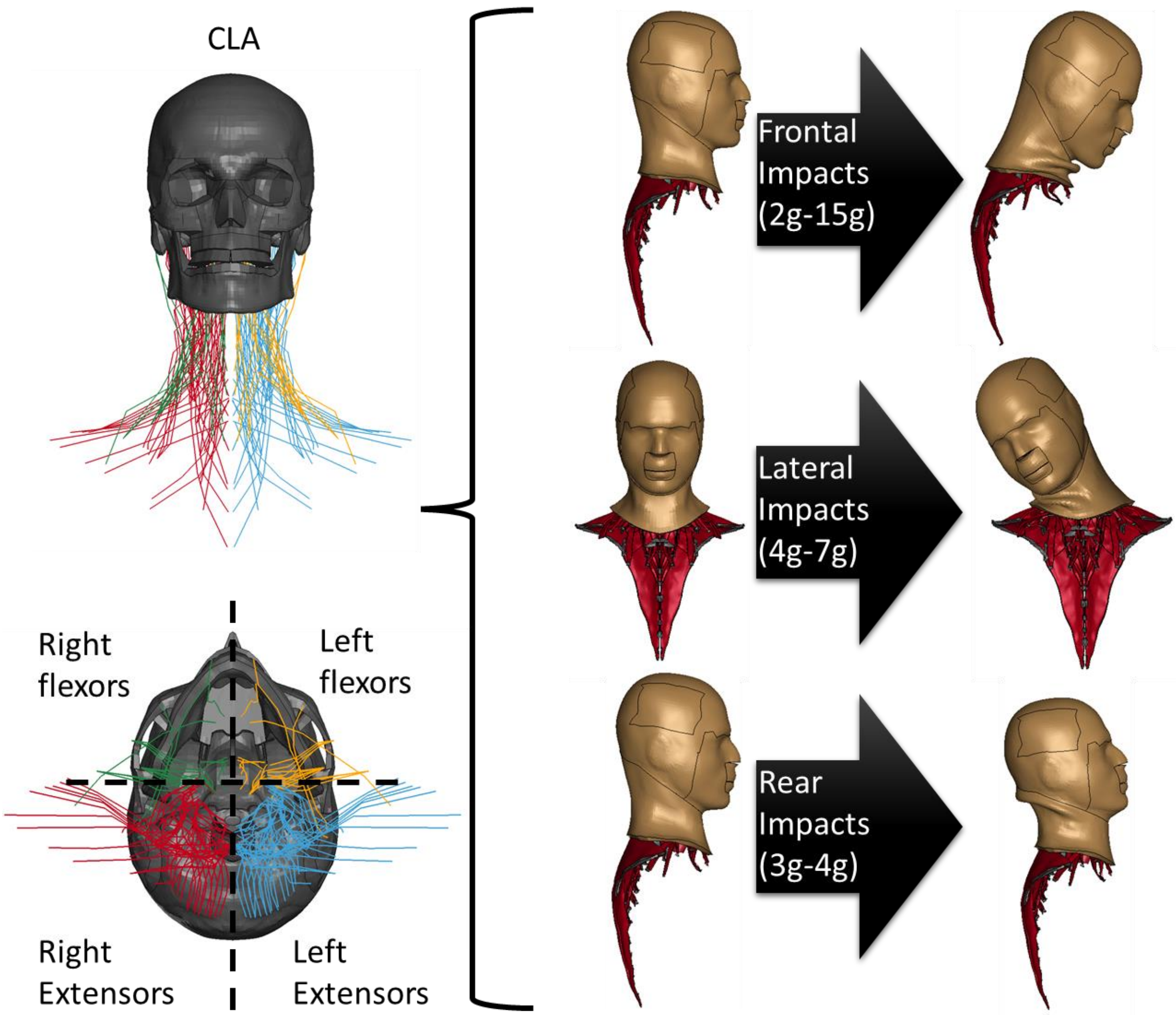

Figure 3: Closed-Loop Activation (CLA) of the four muscle groups (left/right flexors and left/right extensors) were used to simulate the boundary conditions of frontal, lateral, and rear impacts over a range of severities (2g-15g).

Four different lateral impact severities were simulated, ranging from 4g to 7g corresponding to the NBDL volunteer lateral impact sled test maximum accelerations[13,47], for a total duration of 250ms. The average right to left Y-velocity and X-rotational displacement measured at the first thoracic vertebra (T1) in the volunteer experiments were applied to the T1 in the model.

Two rear impact severities were simulated, 3g and 4g, corresponding to sled test accelerations from 12 male volunteers[44], for a total duration of 235ms. The average linear rearward X-acceleration, Z-acceleration, and Y-rotational displacement measured at the first thoracic vertebra (T1) in the volunteer experiments were applied to the T1 in the model.

Closed-Loop Muscle Activation Implementation

With previous literature demonstrating a good potential for a PID controller to model muscle activation[19,22,30], a scheme embedding two PID controllers (Figure 4) was investigated to represent the VCR and CCR reflexes, as reported in experiments with cats, monkeys and humans.[24,39,40,43] The VCR system was represented by a PID controller that monitored head rotational displacements as input while the CCR system was represented by a second PID controller that used muscle stretch as input. The input of the CCR was the sum of the stretches of all active Hill-type beam elements in series at the medial portion of the muscle with the highest volume (capable of producing the highest force) of each muscle group (Figure). These elements were selected after observing which region had the highest deformation in frontal and rear impact simulations, representing the largest expected CCR neuronal signal.

Using MATLAB Simulink (Mathworks, Natick, MA, USA), the VCR and CCR controller parameters were simultaneously calibrated to the OMA activation curves for three frontal impact cases (2g, 8g, and 15g). The experimental head rotation and simulated OMA muscle stretches were defined as the controller input signals. The three impact scenarios were examined simultaneously, and the PID controller parameters were identified based on minimizing the average mean square error between the PID controller and optimized activation curves. It is important to note that the controller was not calibrated to a single impact scenario, and therefore, due to tradeoffs during the optimization process, it was not expected to precisely match any one of the OMA curves. For the VCR, the proportional gain obtained through this methodology was 0.29 and the derivative gain was equal to 1.4. For the CCR, the proportional gain was 0.05 and the derivative gain was equal to 0. The integral gains of both controllers were set to zero, supported by previous research demonstrating adequate controller performance for reflex behavior with only proportional and derivative gains.[41]

A study on decerebrated cats (i.e. no CCR response) identified that the VCR started responding after a head rotation around 5°.[40] Based on this physiological separation of the VCR and CCR, the controller was designed such that if the head rotation measured in all three axes was lower than 5°, only the CCR was actuating. For angles greater than 5°, the CCR and VCR responses were both active. However, the maximum contribution of the CCR to the muscle activation was limited to 10% (f_{CCR}, Figure 4), based on the lowest activation magnitude from the OMA.[10] The VCR could provide a maximum of 90% muscle activation so that the total maximum activation was 100%.

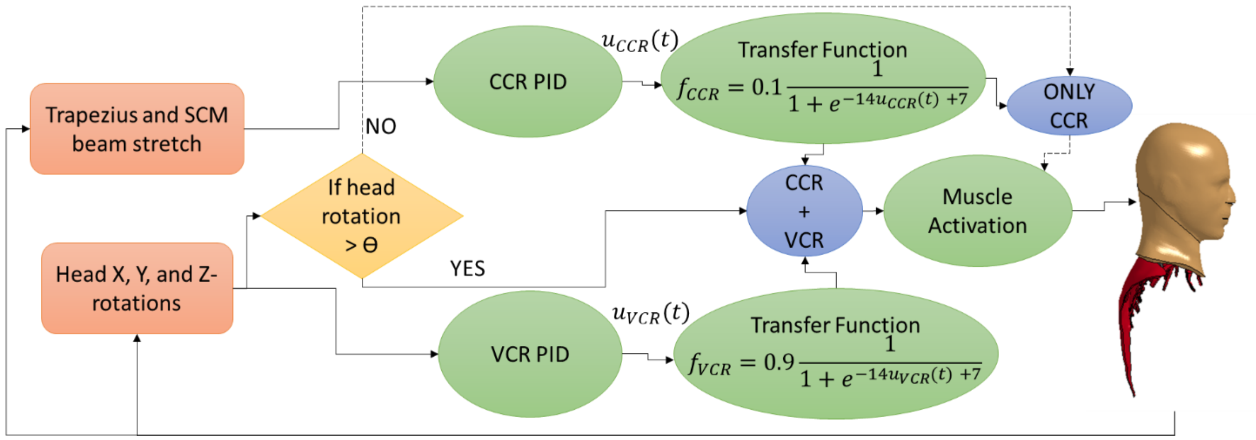

Figure 4: Closed-loop controller flowchart for the extensors, demonstrating the CCR and VCR PID controllers and summation of responses.

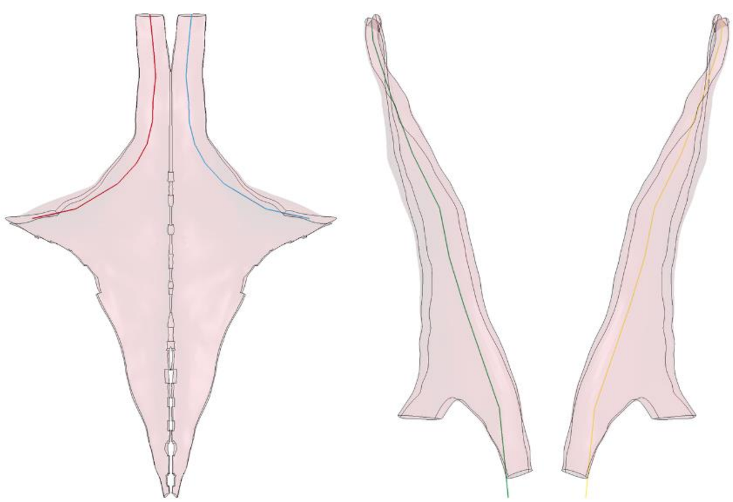

Figure 5: Frontal view of the active muscle fibers (colored lines) used as input for the CCR portion of the control. For the extensors, the lateral fibers of the trapezius were used (left image); and for the flexors, the fibers of the sternocleidomastoid were used (right image).

Previously, it was shown that maintaining an activation ratio of 1:5 between the extensor and flexor muscles improved the kinematic response of the model.[10] Thus, in the current model, the CCR and VCR contribution for the flexors was multiplied by five to maintain this ratio, so that the overall contribution of the flexors to the activation strategy was similar to the extensors. Each one of the four muscle groups received a specific input from the controller based on the change in length of the particular fibers within the monitored muscle. The VCR gains were positive for the antagonistic muscle groups, relative to the head rotation, and negative to the agonist muscles. The CCR gains were positive for lengthening and shortening of the muscles relative to the resting length.

For each of the impact scenarios (Table 1), the proposed closed-loop activation (CLA) scheme was compared to three previous open-loop activation schemes (MMA, CMA, and OMA).[10] The correlation between the activation schemes head kinematics and the experimental data was determined using cross-correlation analysis (CORA, Partnership for Dummy Technology and Biomechanics, R. 3.6.1, Germany).

Table 1: Simulated impact cases with activation schemes, peak sled accelerations, and experimental data sets representing frontal, lateral and rear impact conditions.

Case nomenclature	Muscle activation schemes	Peak sled acceleration (g)	Experimental Data
Frontal (FRT)	Closed-loop: CLA Open-loop: MMA, CMA, OMA	2, 3, 6, 8, 10, 12, 13, 14, 15	NHTSA 2012; Thunnissen et al., 1995[32,47]
Lateral (LAT)	Closed-loop: CLA Open-loop: MMA, CMA, OMA	4, 5, 6, 7	NHTSA 2012; Thunnissen et al., 1995[32,47]
Rear (REA)	Closed-loop: CLA Open-loop: MMA, CMA, OMA	3, 4	Sato et al., 2014[44]

5. Results

The head kinematics obtained for the proposed CLA activation model, for each frontal impact direction and acceleration, were extracted and compared to the human volunteer test results as well as the three open-loop activation schemes (MMA, CMA, OMA) (Figure 4).

The head kinematics resulting from the CLA presented an average cross-correlation rating of 0.667 for frontal impacts, 0.777 for lateral impacts, and 0.690 for rear impacts (Figure 5), comparable to the respective correlation values of 0.691, 0.753, 0.703 for the open-loop CMA results. Average correlation results for all impact cases were within 2% for the CLA (0.699) and CMA (0.709) muscle activation strategies.

The average correlation of the CMA was 9% lower than that of the OMA, where the latter strategy represented the highest possible correlation for the model since the open-loop activation parameters were calibrated for individual impact cases. The MMA presented the lowest average correlation for all impact scenarios, which may be expected since this method was not calibrated or optimized to the experimental data.

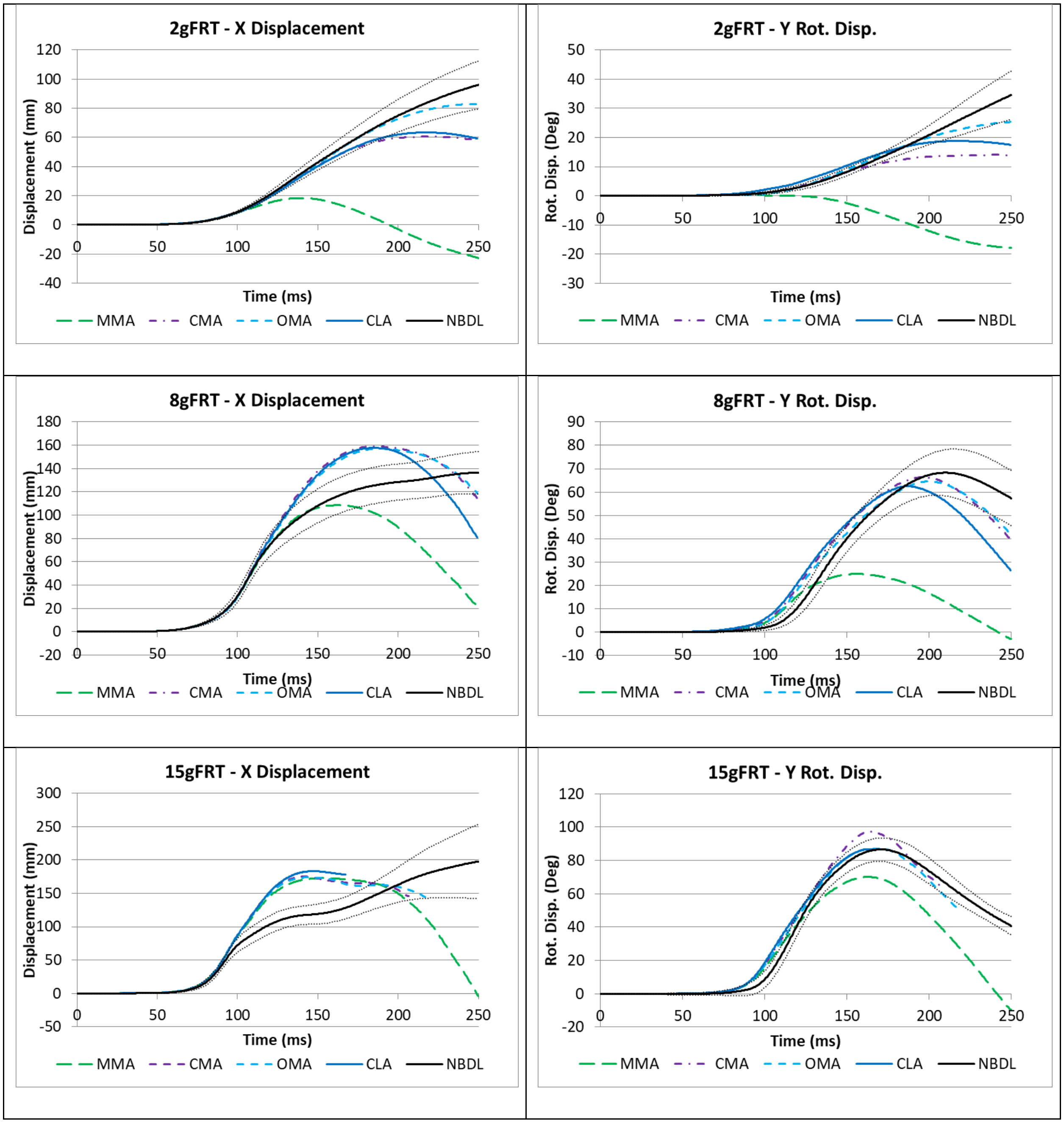

Figure 4: Comparison of the frontal impact head kinematics for the proposed CLA compared to NBDL human volunteer test data average (solid black line) and standard deviation (dotted black line). MMA, CMA, and OMA results are included for reference. The early interruption of the curves for the 15g impact is a result of bone fracture in the model.

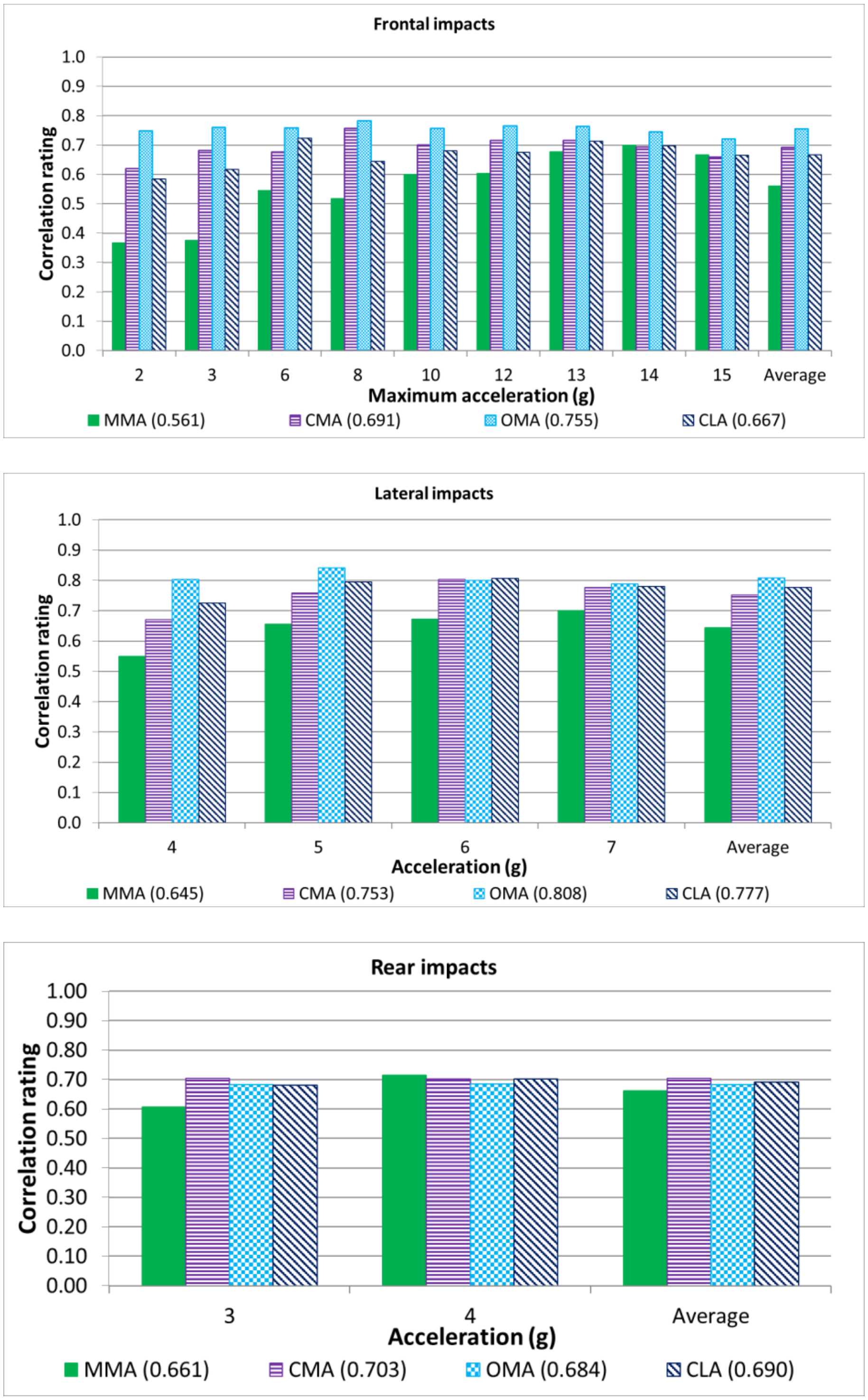

Figure 5: Correlation ratings for the muscle activation schemes (MMA, CMA, OMA, CLA) in frontal, lateral, and rear impacts. The average correlation rating for all cases is shown in brackets.

6. Discussion

Implementation of the head rotation (VCR) and muscle stretch (CCR) reflex responses in a closed-loop muscle controller demonstrated effective performance for simulating neck muscle activation across a broad range of impact scenarios, considering different impact directions and severities. In addition, this was the first study to examine independent assessment of a closed-loop controller for muscle activation over a wide range of impact severities and directions. The CLA scheme developed in this work produced similar head kinematics results to the open-loop CMA scheme.[10] As a single open-loop activation strategy, CMA was based on a known reflex mechanism, compared to the OMA that used a specific activation strategy for each impact case, representing the maximum possible correlation for a given impact direction and severity.

The CLA scheme with two PID controllers resulted in initial activation of the flexors followed by the activation of the extensors, which was observed in frontal and rear impacts with volunteers.[7,11,14,27] However, the opposite was also observed in frontal impacts.[14,28] The order of activation of flexors and extensors was attributed to the CCR reflex implementation that activated the flexors even when they were shortening. The overall CLA correlation was comparable to the CMA but lower than that of the OMA. The calibration of the control parameters using the three frontal impact cases resulted in performance trade-offs; therefore, the CLA activation could not match the correlation rating of the OMA for these specific accelerations. The PID controller is a linear simplification of a complex non-linear reflex system. Although previous studies have identified that a PID controller can generate good approximations to individual impact cases[41], it is evident that these controller parameters would need to be optimized for different impact scenarios. To address this concern, the current study optimized the controller parameters across a wider range of impact severities (2g-15g) and subsequently examined the controller performance across 12 uncalibrated impact conditions.

The CLA also resulted in an activation onset time of up to 90ms relative to the 74ms of the CMA and MMA for the lower severity impacts. For context, the range of activation times of the trapezius and sternocleidomastoid reported in the literature vary from 55 to 99ms in impact tests.[10] Implementing delays in the activation can approximate the neuronal delays in the reflex mechanisms, but the PID parameters also control the activation timing. Therefore, the neuronal delay in this study was considered to be integrated within the PID controller and the overall activation time fell within the range of values presented in the literature.

The CLA scheme presented similar kinematics to the CMA in rear impacts and better-correlated kinematics than the CMA in lateral impacts, which indicates that the model is stable and functional in a variety of impact directions. Furthermore, even with the use of simplified muscle grouping, the CLA obtained a reasonable response in complex cases such as the lateral impacts.

For frontal impacts, the lowest correlation ratings were obtained in the cases with the lowest accelerations. This result was consistent for open-loop and closed-loop activation strategies and may be the result of the skin and adipose tissue having overly stiff properties. The model includes material properties from porcine tissue, which have been suggested to have a stiffer response to shear than the equivalent human tissues.[15] Such findings demonstrate that control parameters and muscle activation strategies may be somewhat model-specific, with no single set of idealized parameters for HBM in general.

The proposed closed-loop controller obtained similar kinematics to current commercial implementations of the CMA open-loop activation in multiple directions and impact severities, while also representing known muscle reflex mechanisms. The new controller may also provide an improved response in multi-directional impact scenarios, which will be the focus of future studies. Importantly, the inclusion of the new closed-loop controller did not significantly increase the computational time of the model, demonstrating a computationally effective solution for multidirectional impacts.

There were three main limitations identified in the present study. First, the stiffness of the soft tissues (skin and adipose tissue) could have had increased the effective stiffness of the neck and affected the resulting global head kinematics, particularly for lower severity impacts. Second, the input of the CCR PID controller (muscle stretch) was taken from a specific row of active Hill-type elements in the midsection of the largest muscle in each muscle group, which may delay or change the activation magnitude in movements that do not stretch this specific muscle region. While not investigated in this study, interactions with seatbelts or a seat headrest may alter the distribution of deformation within the neck and could affect the resulting muscle activation. Third, individual motor units within each muscle are activated independently by a motor neuron, compared to the model with activated each whole muscle group in a similar fashion. However, the resultant head kinematics found in this study indicated adequate approximation for this global analysis as well as reasonable performance trends within the respective muscle groups. The method of using the stretch of the active Hill-type elements of the muscles and head rotation as the input of a CCR and VCR controllers, respectively, could be improved in future work through higher muscle group discretization and more thorough optimization of the controller parameters. However, the presented results indicate that the application of a single controller calibrated only for a few impact cases generated reasonable head kinematics for impacts in three directions and over a wide range of impact severities.

Acknowledgments

Financial support for this research was provided by the Natural Sciences and Engineering Research Council of Canada, Global Human Body Models Consortium, FCA Canada, GM Canada, and Honda R&D Americas; the head-and-neck model provided by the Global Human Body Models Consortium; and computing resources provided by Compute Canada.

Conflict of Interest Statement

The authors have no conflict of interest to declare.

References

1. Albert, D. L., S. M. Beeman, and A. R. Kemper. Evaluation of Hybrid III and THOR-M neck kinetics and injury risk under various restraint conditions during full-scale frontal sled tests. *Traffic Inj. Prev.* 19:S40–S47, 2018.

2. Anderson, J., Z. Li, and F. Goubel. Models of skeletal muscle to explain the increase in passive stiffness in desmin knockout muscle. *J. Biomech.* 35:1315–1324, 2002.

3. Arbogast, K. B., S. Balasubramanian, T. Seacrist, M. R. Maltese, J. F. García-España, T. Hopely, E. Constans, F. J. Lopez-Valdes, R. W. Kent, H. Tanji, and K. Higuchi. Comparison of kinematic responses of the head and spine for children and adults in low-speed frontal sled tests. *Stapp Car Crash J.* 53:329–72, 2009.

4. Barker, J. B., and D. Cronin. Multi-level Validation of a Male Neck Finite Element Model with Active Musculature. *J. Biomech. Eng.* , 2020.doi:10.1115/1.4047866

5. Barker, J. B., D. S. Cronin, and R. W. Nightingale. Lower Cervical Spine Motion Segment Computational Model Validation: Kinematic and Kinetic Response for Quasi-Static and Dynamic Loading. *J. Biomech. Eng.* 139:061009, 2017.

6. Bensamoun, S., L. Stevens, M. J. Fleury, G. Bellon, F. Goubel, and M. C. Ho Ba Tho. Macroscopic-microscopic characterization of the passive mechanical properties in rat soleus muscle. *J. Biomech.* 39:568–578, 2006.

7. Blouin, J. S., M. Descarreaux, A. Bélanger-Gravel, M. Simoneau, and N. Teasdale. Attenuation of human neck muscle activity following repeated imposed trunk-forward linear acceleration. *Exp. Brain Res.* 150:458–464, 2003.

8. Brolin, K., P. Halldin, and I. Leijonhufvud. The effect of muscle activation on neck

response. *Traffic Inj. Prev.* 6:67–76, 2005.

9. Carlsson, A., S. GP, A. Linder, and M. Svensson. Motion of the head and neck of female and male volunteers in rear impact car-to-car tests at 4 and 8 km/h. *IRCOBI Conf. Hanover, Ger. Sept. 2010* 29–40, 2010.

10. Correia, M. A., S. D. McLachlin, and D. S. Cronin. Optimization of muscle activation schemes in a finite element neck model simulating volunteer frontal impact scenarios. *J. Biomech.* , 2020.doi:10.1016/j.jbiomech.2020.109754

11. Dehner, C., S. Schick, M. Kraus, A. Scola, W. Hell, and M. Kramer. Muscle Activity Influence on the Kinematics of the Cervical Spine in Frontal Tests. *Traffic Inj. Prev.* 14:607–613, 2013.

12. Ejima, S., K. Ono, K. Kaneoka, and M. Fukushima. Development and Validation of the Human Neck Muscle Model Under Impact Loading. *Ircobi* 245–255, 2005.

13. Ewing, C. L., and D. J. Thomas. Human Head and Neck Response To Impact Acceleration. *DTIC Doc.* , 1972.

14. Fanta, O., D. Hadraba, F. Lopot, P. Kubový, J. Bouček, and K. Jelen. Pre-activation and muscle activity during frontal impact in relation to whiplash associated disorders. *Neuroendocrinol. Lett.* 34:708–716, 2013.

15. Gepner, B. D., H. Joodaki, Z. Sun, M. Jayathirtha, T. Kim, J. L. Forman, and J. R. Kerrigan. Performance of the obese GHBMC models in the sled and belt pull test conditions IRCOBI co. *Conf. Proc. Int. Res. Counc. Biomech. Inj. IRCOBI* 2018-Septe:355–368, 2018.

16. Happee, R., E. de Bruijn, P. A. Forbes, and F. C. T. van der Helm. Dynamic head-

neck stabilization and modulation with perturbation bandwidth investigated using a multisegment neuromuscular model. *J. Biomech.* 58:203–211, 2017.

17. Hedenstierna, S., P. Halldin, and K. Brolin. Evaluation of a combination of continuum and truss finite elements in a model of passive and active muscle tissue. *Comput. Methods Biomech. Biomed. Engin.* 11:627–639, 2008.

18. Hedenstierna, S., P. Halldin, and G. P. Siegmund. Neck Muscle Load Distribution in Lateral , Frontal , and Rear-End Impacts A Three-Dimensional Finite Element Analysis. *Spine (Phila. Pa. 1976).* 34:2626–2633, 2009.

19. Ivancic, A., and V. Pradhan. The influence of isometrically derived neck muscle spatial tuning patterns on head response in dynamic conditions. , 2017.

20. Iwamoto, M. Modeling Passive and Active Muscles. Elsevier Inc., 2018, 447–468 pp.doi:10.1016/B978-0-12-809831-8.00011-8

21. Iwamoto, M., Y. Nakahira, H. Kimpara, T. Sugiyama, and K. Min. Development of a human body finite element model with multiple muscles and their controller for estimating occupant motions and impact responses in frontal crash situations. *Stapp Car Crash J.* 56:231–68, 2012.

22. Kato, D., H. Kimpara, Y. Nakahira, and M. Iwamoto. Effects of Controlled Muscle Activations on Human Head–Neck Responses during Low-Speed Rear Impacts. *IRCOBI Proc.* 33–34, 2016.

23. Kato, D., Y. Nakahira, and M. Iwamoto. A study of muscle control with two feedback controls for posture and reaction force for more accurate prediction of occupant kinematics in low-speed frontal impacts. 1–11, 2017.

24. Keshner, E. A. Head-trunk coordination during linear anterior-posterior translations. *J. Neurophysiol.* 89:1891–1901, 2003.

25. Kleinbach, C., O. Martynenko, J. Promies, D. F. B. Haeufle, J. Fehr, and S. Schmitt. Implementation and validation of the extended Hill-type muscle model with robust routing capabilities in LS-DYNA for active human body models. *Biomed. Eng. Online* 16:1–28, 2017.

26. Kumar, S., R. Ferrari, and Y. Narayan. Electromyographic and Kinematic Exploration of Whiplash-Type Neck Perturbations in Left Lateral Collisions. *Spine (Phila. Pa. 1976).* 29:650–659, 2004.

27. Kumar, S., R. Ferrari, and Y. Narayan. The effect of trunk flexion in healthy volunteers in rear whiplash-type impacts. *Spine (Phila. Pa. 1976).* 30:1742–1749, 2005.

28. Kumar, S., Y. Narayan, and T. Amell. Analysis of low velocity frontal impacts. *Clin. Biomech.* 18:694–703, 2003.

29. Le, P., A. Aurand, T. M. Best, S. N. Khan, E. Mendel, and W. S. Marras. An Exploratory Electromyography-Based Coactivation Index for the Cervical Spine. *Hum. Factors* 60:68–79, 2018.

30. Meijer, R., J. Broos, H. Elrofai, E. de Brujin, P. Forbes, and R. Happee. Modelling of Bracing in a Multi-Body Active Human Model IRCOBI. , 2013.at <http://www.ircobi.org/wordpress/downloads/irc13/pdf_files/67.pdf>

31. Meyer, G. A., A. D. McCulloch, and R. L. Lieber. A nonlinear model of passive muscle viscosity. *J. Biomech. Eng.* 133:1–9, 2011.

32. NHTSA. National Highway Traffic Safety Administration. , 2012.at <https://www-nrd.nhtsa.dot.gov/database/VSR/bio/QueryTest.aspx>

33. Ólafsdóttir, J. M., J. K. H. Östh, J. Davidsson, and K. B. Brolin. Passenger Kinematics and Muscle Responses in Autonomous Braking Events with Standard and Reversible Pre-tensioned Restraints. *Int. Res. Counc. Biomech. Inj. Conf.* 46:602–617, 2013.

34. Olszko, A. V, C. M. Beltran, K. B. Vasquez, J. S. McGhee, V. C. Chancey, N. Yoganandan, F. A. Pintar, and J. L. Baisden. Initial analysis of archived non-human primate frontal and rear impact data from the biodynamics data resource. *Traffic Inj. Prev.* 19:S44–S49, 2018.

35. Ono, K., K. Kaneoka, A. Wittek, and J. Kajzer. Cervical Injury Mechanism Based on the Analysis of Human Cervical Vertebral Motion and Head-Neck-Torso Kinematics During Low Speed Rear Impacts. *SAE Tech. Pap. Ser.* 1:, 1997.

36. Östh, J., K. Brolin, and R. Happee. Active muscle response using feedback control of a finite element human arm model. *Comput. Methods Biomech. Biomed. Engin.* 15:347–361, 2012.

37. Östh, J., J. Davidsson, B. Pipkorn, and L. Jakobsson. Muscle Activation Strategies in Human Body Models for the Development of Integrated Safety. *ESV - 24th Int. Tech. Conf. Enhanc. Saf. Veh.* 1–15, 2015.

38. Panzer, M. B., J. B. Fice, and D. S. Cronin. Cervical spine response in frontal crash. *Med. Eng. Phys.* 33:1147–1159, 2011.

39. Peng, G. C. Y., T. C. Hain, and B. W. Peterson. A dynamical model for reflex

activated head movements in the horizontal plane. *Biol. Cybern.* 75:309–319, 1996.

40. Peterson, B. W., J. Goldberg, G. Bilotto, and J. H. Fuller. Cervicocollic reflex: Its dynamic properties and interaction with vestibular reflexes. *J. Neurophysiol.* 54:90–109, 1985.

41. Putra, I. P. A., J. Iraeus, F. Sato, M. Y. Svensson, A. Linder, and R. Thomson. Optimization of Female Head–Neck Model with Active Reflexive Cervical Muscles in Low Severity Rear Impact Collisions. *Ann. Biomed. Eng.* , 2020.doi:10.1007/s10439-020-02512-1

42. Putra, I. P. A., J. Iraeus, R. Thomson, M. Y. Svensson, A. Linder, and F. Sato. Comparison of control strategies for the cervical muscles of an average female head-neck finite element model. *Traffic Inj. Prev.* 20:S116–S122, 2019.

43. Reynolds, J. S., and G. T. Gdowski. Head movements produced during whole body rotations and their sensitivity to changes in head inertia in squirrel monkeys. *J. Neurophysiol.* 99:2369–2382, 2008.

44. Sato, F., T. Nakajima, K. Ono, M. Svensson, K. Brolin, and K. Kaneoka. Dynamic cervical vertebral motion of female and male volunteers and analysis of its interaction with head/neck/torso behavior during low-speed rear impact. , 2014.at <http://www.scopus.com/inward/record.url?eid=2-s2.0-84915781100&partnerID=MN8TOARS>

45. Siegmund, G. P., J.-S. Blouin, J. R. Brault, S. Hedenstierna, and J. T. Inglis. Electromyography of Superficial and Deep Neck Muscles During Isometric, Voluntary, and Reflex Contractions. *J. Biomech. Eng.* 129:66, 2007.

46. Stemper, B. D., and B. D. Corner. Whiplash-Associated Disorders: Occupant Kinematics and Neck Morphology. *J. Orthop. Sport. Phys. Ther.* 46:834–844, 2016.

47. Thunnissen, J., J. Wismans, C. L. Ewing, and D. J. Thomas. Human Volunteer Head-Neck Response in Frontal Flexion: A New Analysis. , 1995.

48. Toursel, T., L. Stevens, H. Granzier, and Y. Mounier. Passive tension of rat skeletal soleus muscle fibers: Effects of unloading conditions. *J. Appl. Physiol.* 92:1465–1472, 2002.

49. Vasavada, A., S. Li, and S. Delp. Influence of muscle morphology and moment arms on moment-geneating capacity of human neck muscles. *Spine (Phila. Pa. 1976).* 23:412–422, 1998.

50. Wismans, J., H. van Oorschot, and H. Woltring. Omni-Directional Human Head-Neck Response. *SAE Trans.* 95:819–837, 1986.

51. Yang, K. H., J. Barker, D. S. Cronin, D. Gierczycka, J. Hu, M. Iwamoto, X. Jin, A. Kalra, H. Mao, B. R. Presley, D. Shen, D. Singh, and F. Zhu. Basic Finite Element Method as Applied to Injury Biomechanics. Elsevier, 2018.doi:10.1016/C2015-0-06702-8

52. Zhang, C., X. Meng, D. E. Anderson, W. Wang, X. Tao, and B. Cheng. Effects of stretch reflex on back muscle response during sinusoidal whole body vibration in sitting posture: A model study. *Int. J. Ind. Ergon.* 71:103–110, 2019.